ACS ENGINEERING Au
AN OPEN ACCESS JOURNAL OF THE AMERICAN CHEMICAL SOCIETY

pubs.acs.org/engineeringau
Article

Synergistic Removal of Cr(VI) with Stable Nanozerovalent Iron Particles and Ultrasound Assistance in the Presence of Organic Additives

Published as part of ACS Engineering Au virtual special issue "Insights, Innovations, and Intensification."

Lucia Cancelada, Jorge M. Meichtry, Hugo Destaillats, and Marta I. Litter*

Cite This: https://doi.org/10.1021/acsengineeringau.4c00011
Read Online

ACCESS | Metrics & More | Article Recommendations | Supporting Information

ABSTRACT: Commercial stable zerovalent iron nanoparticles (nZVI) (NSTAR, not activated) combined with ultrasound (US) were tested for Cr(VI) reductive removal (0.3 mM, pH 3, Fe/Cr molar ratio of 3:1) in the presence of the carboxylic acids (CAs) ethylenediaminetetraacetic acid (EDTA, 1 mM) or citric acid (Cit, 2 mM), in a system open to the air. No Cr(VI) decay up to 180 min was observed under US when only NSTAR nanoparticles were used, while other previously tested commercial nZVI (N25) showed about 40% decay in a few minutes but without further Cr(VI) removal. The addition of EDTA and Cit enabled Cr(VI) removal with NSTAR in the absence of US without prior activation of the particles. A pseudo zero-order kinetics was followed, yielding 32 and 49% removal with EDTA and Cit, respectively. When US was applied, these values almost doubled, reaching 59 and 88% for EDTA and Cit, respectively. A mechanism for Cr(VI) decay was proposed. The present results indicate that the simultaneous use of US and CAs allows for a synergistic Cr(VI) removal by NSTAR avoiding the need of an activation step of the nanoparticles, with a more effective result of Cit compared with EDTA.

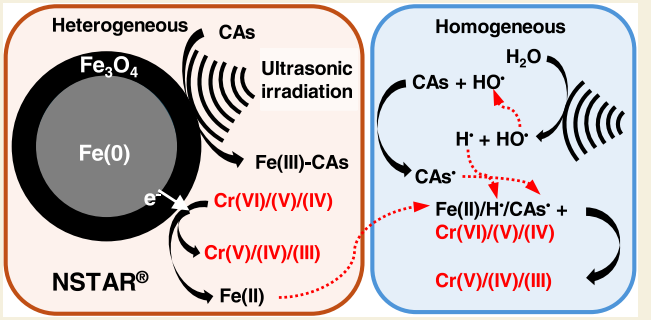

KEYWORDS: *nanozerovalent iron, ultrasound, hexavalent chromium, ethylenediaminetetraacetic acid, citric acid*

1. INTRODUCTION

Water pollution by hexavalent chromium (Cr(VI)) is related to the discharge of wastewaters from industrial processes such as electroplating, leather tanning, industrial painting, mining, or energy generation;[1,2] Cr(III) oxidation was also reported to contribute to the presence of Cr(VI) in some environments.[3] Due to its acute toxicity, its carcinogenic and mutagenic effects, as well as a significant mobility in water, Cr(VI) is considered a priority water pollutant.[4] The World Health Organization (WHO) established in 2011 a maximum allowable concentration for total chromium (Cr_T) in drinking water at 50 $\mu g\ L^{-1}$.[5] Lately, the Office of Environmental Health Hazard Assessment (OEHHA) in California, USA, has published a Public Health Goal (PHG) of 0.02 $\mu g\ L^{-1}$.[6] Discharge limits for Cr_T and Cr(VI) concentrations in wastewaters of several European countries are in the range 0.05−2.00 mg L^{-1}.[1] Cr(VI) treatment usually involves a reduction step to Cr(III), which not only is far less toxic but also a human essential trace metal.[1] Besides, Cr(III) can be easily removed from the solution as a solid after neutralization. However, chemical reduction of Cr(VI) is a costly process demanding significant doses of high-value reductants alongside with the production of substantial quantities of hazardous sludge, hence the need for expensive and proper disposal methods.[1,7,8] For this reason, advanced oxidation/reduction processes (AOPs/ARPs), such as heterogeneous photocatalysis, Fenton and photo-Fenton reactions, ultrasound (US) or the use of zerovalent iron (ZVI), either macro-, micro-, or nanosized, have been investigated for several years as innovative methods for Cr(VI) removal from wastewaters.[9−15]

ZVI has been used as a reducing agent to transform pollutants in wastewater, especially for recalcitrant organic compounds (e.g., halogenated olefins such as trichloroethylene) and metal/metalloid ions (e.g., Cr(VI), As(III/V)).[16] In recent years, zerovalent iron nanoparticles (nZVI) have proved to be relevant because of their excellent properties: the small diameter (10−100 nm) enhances the surface area and thus the chemical reactivity. nZVI exhibits a

Received: March 12, 2024
Revised: May 29, 2024
Accepted: May 29, 2024

typical core−shell structure, with a nucleus of zerovalent iron and an external Fe(II)/Fe(III) oxide shell, as a result of the corrosion and oxidation of metallic iron. The outer layer acts not only as a protection for the reactive nucleus but also as an adsorptive surface for pollutants that can participate in charge transfer processes between Fe^0 and species in aqueous solution.[17,18]

The reduction of Cr(VI) using nZVI has been the subject of extensive research, as described before,[7,19−21] including works from our group.[18,22] However, the low stability and tendency to aggregate via van der Waals and magnetic attraction forces are primary drawbacks in the utilization of nZVI for the removal of aqueous Cr(VI).[1,23] NSTAR is a commercially available, surface-stabilized nZVI product, consisting in a Fe^0 core protected by a thin inorganic layer that prevents against nZVI rapid oxidation. According to the manufacturers, NSTAR is easier and safer to store, transport, handle, and process compared to nonstabilized nZVI, while keeping its chemical reactivity and ability to reduce pollutants.[24] The product is usually activated before use and several procedures have been tested such as prior heating or dispersion in water.[25,26]

On the other hand, the exposure of water to ultrasound (US) results in local hot spots (4000−5000 K) due to the formation, growth, and collapse of cavitation bubbles containing entrapped gases and vapors. At collapse, the thermolytic decomposition of bubbles generates free radical species that promote the oxidation or reduction of dissolved solutes at the gas−liquid interface or in the bulk liquid. Equations (S1−S11) in the Supporting Information (SI) show a simplified set of reactions taking place in sonochemical aqueous systems under argon and in air,[27] where the main species produced are $HO^•$, $H^•$, $HO_2^•$, and H_2O_2. Since these species can participate in the transformation of pollutants, this system is considered an AOP/ARP[28] as well as a green technology because it does not require additional chemicals.[27] In previous papers,[10,11] our group analyzed the reduction of Cr(VI) (0.3 mM, pH 2) using 850 kHz ultrasound in the presence of carboxylic acids (CAs), such as citric acid (Cit) and ethylenediaminetetraacetic acid (EDTA), under different atmospheres. It was concluded that the complete Cr(VI) reduction after 180 min was obtained only in the presence of EDTA and Cit under argon bubbling or with the reactor open to air. Nonvolatile water−soluble substances like these CAs, which do not partition to the vapor phase or the bubble interface in the US system, remain in the aqueous phase and are degraded by oxidative species produced at the cavitation bubble (such as $HO^•$), which migrate out into bulk solution and generate reducing secondary radicals ($R^•$, eq (S10) and $ROO^•$, eq (S11)). A complete mechanism regarding the ultrasonic reduction of Cr(VI) has been proposed in these papers.[10,11] This mechanism involves the action of H_2O_2 and reducing organic radicals eventually leading to the formation of Cr(V), Cr(IV), and Cr(III), the final stable species.

The combination of US and ZVI for the transformation of pollutants was reported as early as 1998, when Hung and Hoffmann showed that the reductive degradation of CCl_4 by elemental iron in Ar-saturated solutions was enhanced by the presence of US.[29] Literature reports indicate that the combination of US with iron in three states (i.e., Fe^0, Fe^{2+}, and Fe^{3+}) improves the degradation of pollutants.[30] The presence of Fe^0 leads to an increase in the cavitation intensity by acting as nuclei for surface cavitation, proportionately increasing the number of cavitation events. Additionally, US can increase the reactivity of the nanoparticles by rupturing aggregates, diminishing the particle size, and removing corrosion products that could passivate the metallic surface.[14] Lastly, the turbulent conditions created by sound waves improve the mass transfer of reactants to the nZVI surface. All of these phenomena can cause a dramatic increase on the nZVI pollutant removal efficiency, therefore lowering the reaction times and/or nZVI doses.[14,31]

Although the combination of sonolysis with nZVI for the treatment of pollutants presents several examples in the literature,[31−36] only four publications refer to Cr(VI) reduction by the US-nZVI combination and report an improvement on Cr(VI) removal rate and/or capacity.[14,15,31,35] The parameters affecting the Cr(VI) removal, such as US frequency, power, temperature, initial pH, and Cr(VI) concentration, were investigated and a mechanism was proposed.[31] Another paper studied the Cr(VI) removal with a nZVI material prepared using US (20 kHz) during the synthesis; these nanoparticles had a higher specific surface area compared with the ones prepared in the absence of US and have been found very effective for Cr(VI) removal.[37]

In the present paper, the application of NSTAR for Cr(VI) reduction with US assistance in the presence of EDTA or Cit as additives under air bubbling has been studied. NSTAR powder is a different material from those previously tested in combination with US.[14,15,35] Another commercial nZVI suspension (N25)[38] was also tested for comparison, and a mechanism is proposed.

2. MATERIALS AND METHODS

2.1. Chemicals and Materials

Potassium dichromate (99.9%, Merck), sulfuric acid (98%, Merck), hydroquinone (≥99%, Merck), citric acid monohydrate (99%, Riedel de Haën), disodium EDTA dihydrate (99.0%, Mallinckrodt), perchloric acid (70%, Biopack) for pH adjustments, 1,5-diphenylcarbazide (DFC, ACS, Biopack), 1,10-phenantroline monohydrate (ACS, Biopack), sodium acetate (≥99.0%, Biopack), acetone (≥99.5%, Sintorgan), and potassium iodide (99.6%, Anedra) were used. All solutions and suspensions were prepared with Milli-Q grade water (resistivity = 18 MΩ cm at 25 °C, Osmoion Apema). NANOFER STAR and NANOFER 25 (hereafter NSTAR and N25, respectively) were supplied by NANOIRON, s.r.o. (Czech Republic). NSTAR was provided as an air-stable powder[24] and kept at a low temperature (4−8 °C) until used, while N25 was provided as a suspension in water.[38]

2.2. Characterization of the Zerovalent Iron Nanoparticles

Although NSTAR characterization was reported elsewhere,[33,39−41] some of their properties may change from batch to batch. Fe^0 content was determined by measuring the hydrogen gas evolved during particle digestion in concentrated H_2SO_4;[42] the mass percentage of total Fe (Fe_T) in NSTAR was obtained after Fe_T measurement (see Section 2.5) in the digested sample. The X-ray diffraction (XRD) pattern was obtained using a PanAnalytical Empirean X-ray diffractometer equipped with a PIXcel 3D detector. Cu−Kα radiation was used over a 2θ range of 10−90°, with a step size of 0.0394°. The Raman spectrum was obtained with a LabRAM HR Raman system (Horiba Jobin Yvon), equipped with a confocal microscope, two monochromator gratings, and a charge-coupled device detector, using the He−Ne laser line at 632.8 nm as the excitation source. The Mössbauer spectrum was obtained at room temperature in a conventional constant acceleration spectrometer in transmission geometry with a ^{57}Co/Rh source. The velocity range was set between −10 and 10 mm s^{-1}. The fitting of the spectra was performed using the Normos software, and the isomeric shift was assigned according to the α-Fe reference. The specific surface area was determined by the

https://doi.org/10.1021/acsengineeringau.4c00011
ACS Eng. Au XXXX, XXX, XXX−XXX

Brunauer–Emmett–Teller method with a Micromeritics AutoPore IV 9500 Series instrument. Samples were previously degassed for 2 h at 70 °C. N_2 at 77 K was used as the adsorbent. The NSTAR batch was not activated in any case for the characterization or the Cr(VI) removal experiments.

The properties of the N25 nanoparticles were previously reported by the manufacturers and by our group.[18,38]

2.3. Sonochemical Reactor Design

The sonochemical reactor (see Figure S1 in the Supporting Information (SI), Section S2), consisting of a 32 mm outer diameter, 2 mm thick and 400 mm high borosilicate tube, 250 mL total volume (1), was placed into a UST 02 Laboratory Reactor (Meinhardt-Ultraschalltechnik, Leipzig, Germany) filled with 900 mL of water (2). An 850-kHz E/805/T02 ultrasonic transducer powered by a K 8 ultrasonic power generator (Meinhardt-Ultraschalltechnik, Leipzig, Germany) (3) was attached with a DN 60 flange to the bottom of the UST 02 reactor. In this configuration, the transducer was in direct contact with water but not with the contents of the sonochemical reactor. As a result, the chemical interaction between the reactive nanoparticles and the transducer surface, i.e., corrosion, was avoided. An external jacket (4) allowed water circulation and maintained the temperature at 25 °C. A silicone tube (4 mm-diameter) entering from the top (5) allowed bubbling air (0.5 L min^{-1}), which was used for agitation inside the sonochemical reactor. A ceramic air diffuser (6) was set in the bottom of the tube. The suspension of nZVI containing dissolved Cr(VI) (7) was poured into the reaction tube.

The total power input by the transducer into the liquid inside the sonochemical reactor (P_{ac}) was determined by calorimetry.[43] A value of $P_{ac} = 35 \pm 2$ W L^{-1} was obtained. Potassium iodide oxidation[44] was used to evaluate the yield of generation of hydroxyl radicals ($HO^{\bullet}$) inside the sonochemical reactor under the same conditions (temperature, pH, air bubbling) used in the experiments. At pH 3, a $HO^{\bullet}$ generation rate of $(3.2 \pm 0.2) \times 10^{-6}$ mol L^{-1} min^{-1} was obtained; if this value is divided by the input power, an $HO^{\bullet}$ generation yield of $(1.5 \pm 0.2) \times 10^{-9}$ mol J^{-1} was obtained.

2.4. Sonochemical Experiments

The experiments were performed with 200 mL of 0.3 mM Cr(VI) solution in the presence of NSTAR, using a Fe_T/Cr molar ratio (MR) of 3:1, Cit (2 mM) or EDTA (1 mM), at pH 3, and under air bubbling and 30 °C. Under these conditions, Cr(VI) is almost exclusively found as the $HCrO_4^-$ species.[1,2] Changes on pH at the end of the reaction were negligible. All experiments were performed at least by duplicate and the relative standard deviation among replicates was never higher than 10%. The fitting of the experimental points was performed with the Origin 9.0 software.

2.5. Analytical Determinations

Samples (1 mL) were periodically taken from the sonochemical reactor and centrifuged in an Eppendorf MiniSpin centrifuge at 13 400 rpm for 2 min. Then, 0.2 mL aliquots of the supernatant were taken for Cr(VI), Fe(II), and Fe_T analysis. Cr(VI) was determined spectrophotometrically by the DFC method at 540 nm.[45] Fe_T and Fe(II) were measured using the *o*-phenanthroline method at 508 nm.[46] All UV–vis absorption measurements were performed employing a PG Instruments UV–visible spectrophotometer, model T80+.

3. RESULTS AND DISCUSSION

3.1. NSTAR Characterization

The properties of the NSTAR nanoparticles of the batch used here are presented in Table 1. The data were compared with those reported by the manufacturers,[24,39,47] by other authors,[18,25,32,33,40,41,48] and with those of N25.[18,38]

Figure 1 shows the XRD pattern of the present NSTAR sample, where the α-Fe phase can be clearly distinguished, indicating that the original material is essentially Fe^0 (2θ = 44.72, 65.05, and 82.36°).[13,25,26,31,33,39–41,47] Another minor signal at ≈36° could be assigned to iron oxides, such as magnetite or maghemite.[25,31,39–41,47]

Although magnetite or maghemite cannot be differentiated by XRD, the Raman spectrum of the sample (Figure 2) indicates that the iron oxide present in the sample is magnetite.

Figure 3 shows the Mössbauer spectrum. Using the Normos program[49] with a constant Lamb–Mössbauer factor, it can be estimated that 95% of the Fe present corresponds to Fe^0. The spectrum shows a minor contribution of superparamagnetic Fe (Fe SPM), attributable to nanometric iron oxides and to some minor impurities, probably generated from the NSTAR synthesis procedure. The signals observed in the Fe SPM spectra may be indicative of magnetite, confirming the Raman results.

These analysis suggests that NSTAR nanoparticles present a Fe^0-rich core with a magnetite-rich shell and is compatible with the description provided by the supplier[39,47] and observed by other authors:[40,41] the surface of the nanoparticles is stabilized by a thin layer of iron oxide, which prevents further oxidation after contact with atmospheric oxygen.

Table 1. Properties of Commercial Iron Nanoparticles (NSTAR and N25)

sample	Fe_T	Fe^0 (%)	S_{BET} (m^2 g^{-1})	ref
NSTAR (solid)	0.85 ± 0.02 mg mg^{-1}	68 ± 6[a], 95[b]	21.9 ± 0.4	this work
NSTAR (solid)		78[a,c],77[a,d]	14.6[c], 30.0[d]	25
NSTAR (solid)			15.5	33
NSTAR (solid)		>90[e]		48
NSTAR (solid)		76[f], 91[e]	18.5	40
NSTAR (solid)		69.0 ± 3.4[a]	17.0 ± 0.8	41
NSTAR (solid)		72–85[g]	>25	47
NSTAR (solid)		≥70[g]		24
N25 (water suspension)	242 g L^{-1}	80–85[g]	20–25	18,38

[a]Calculated from H_2 generation experiments. [b]Determined from Mössbauer analysis (see Section 3.1). [c]Nonactivated batch. [d]Activated batch. [e]Calculated from XRD analysis. [f]Calculated from Mössbauer analysis. [g]Analytical method not indicated.

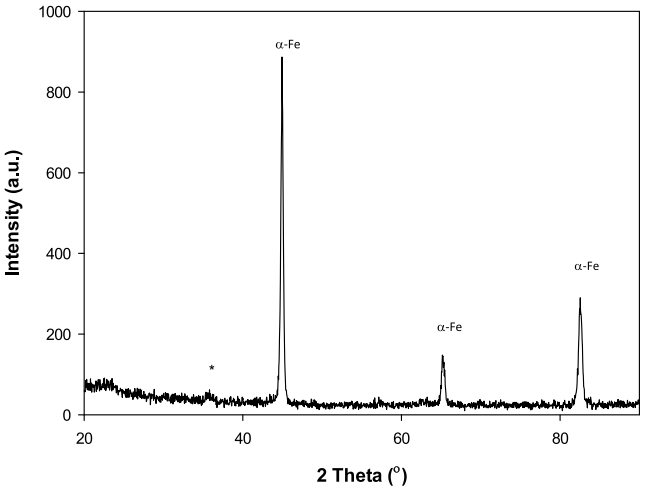

Figure 1. XRD pattern of NSTAR nanoparticles. α-Fe reference peaks are indicated. The asterisk (*) indicates a signal that could be assigned to magnetite or maghemite.

https://doi.org/10.1021/acsengineeringau.4c00011
ACS Eng. Au XXXX, XXX, XXX–XXX

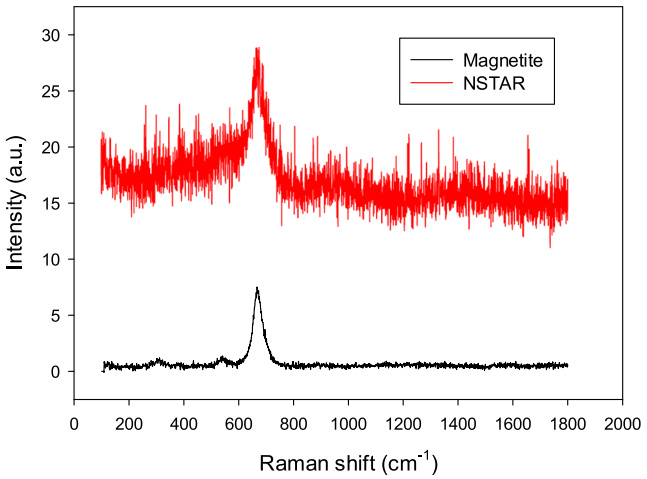

Figure 2. Raman spectrum of NSTAR nanoparticles. The magnetite spectrum is also shown as reference.

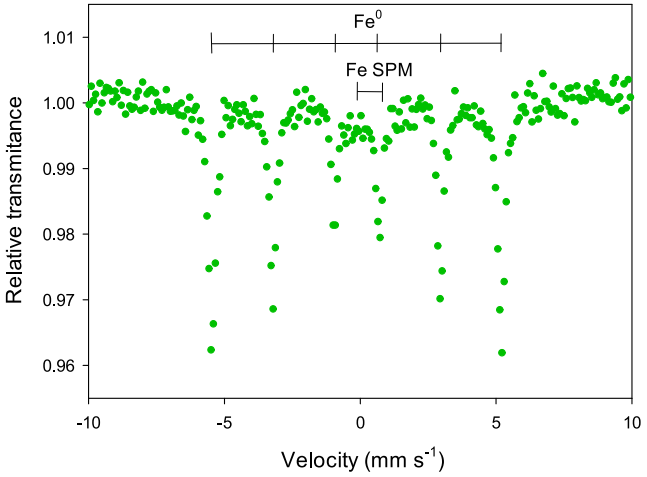

Figure 3. Mössbauer spectrum of NSTAR nanoparticles. Fe^0 represents the characteristic signals of zerovalent iron and Fe SPM those of superparamagnetic iron.

3.2. REMOVAL OF CR(VI)

In Figure 4, results of the Cr(VI) (0.3 mM) ultrasonic decay in the presence of NSTAR without additives and in the presence of Cit (2 mM) or EDTA (1 mM) at pH 3 are shown. These conditions, with the exception of the pH, were similar to those used in previous works of Cr(VI) removal by TiO_2 photocatalysis[50] and US.[10,11] The pH used here was the optimum value found in previous works from the group on Cr(VI) removal by zerovalent iron nanoparticles.[18,22] Although lower pH values would favor the removal of the NSTAR passivating layers (i.e., the external iron oxides), releasing Fe to the solution,[51] undesired corrosion reactions (e.g., H_2 generation that consumes Fe^0 without contributing to the Cr(VI) reduction) could also take place. The concentration of Cit (2 mM) was the optimum value found in the TiO_2/Cr(VI) photocatalytic system studied before,[50] while the concentration of EDTA (1 mM) was selected to correspond approximately to the same initial total organic carbon (TOC) of Cit. The nanoparticles were added to the system at a Fe_T/Cr MR of 3:1 and then sonication was initiated (t = 0) using air bubbling agitation to avoid the settling of the nanoparticles and to enhance the solution mixing. As said, changes on pH at the end

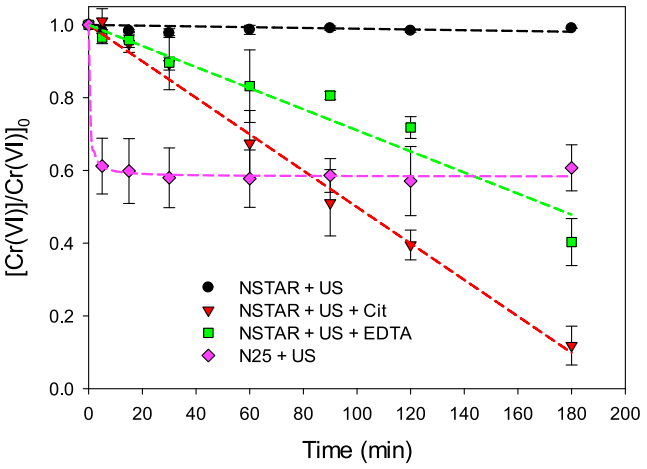

Figure 4. Temporal profile of normalized Cr(VI) concentration ($[Cr(VI)]/[Cr(VI)]_0$) during the sonochemical experiments in the presence of NSTAR, NSTAR + Cit, NSTAR + EDTA, and N25. Conditions: $[Cr(VI)]_0$ = 0.3 mM, Fe_T/Cr MR 3:1, pH 3, T = 30 °C, air bubbling agitation, [Cit] = 2 mM, [EDTA] = 1 mM. Linear fittings are presented except for the experiment with N25, where the fitting corresponds to a pseudo-second-order kinetics (see later, eq 1).

of the reactions were negligible, effect that was observed also in previous experiments with Cr(VI) under US.[10] Both Cr(VI) thermal reduction by Cit or EDTA (in the absence of US and nanoparticles) and sonochemical reduction in the absence of nZVI and CAs were negligible (results not included). This has also been observed in our previous work[10] and indicates that Cr(VI) reduction with CAs only takes place under US.

Figure 4 shows no Cr(VI) decay after 180 min when only NSTAR and US were used. When N25 was used instead of NSTAR, a 40% removal was obtained almost instantaneously, but then the reaction stopped. Interestingly, in a previous work from our group,[18] almost complete Cr(VI) removal was obtained with N25 in the absence of sonication under the same conditions; the difference can be ascribed to a less efficient mixing, or to a deleterious effect caused by US, probably by damaging the N25 nanoparticles. Also, a side reaction, e.g., H_2 generation and/or O_2 reduction[32,33,35] could be responsible for the unproductive oxidation of Fe^0. Other authors reported that US increased the Cr(VI) removal capacity of nZVI at pH 3,[31] although the nZVI material used there was less reactive than N25.[18]

With the addition of CAs, the Cr(VI) removal rate with NSTAR was greatly enhanced to 59% with EDTA and to 88% with Cit. The model fitting in Figure 4 shows an almost constant decay rate. Zhou et al. also observed an improvement of the removal of Cr(VI) with borohydride-prepared nZVI after the addition of sodium citrate.[52] For N25, a pseudo-second-order kinetic model[8] was tested according to eq 1

$$q = \frac{k_a \times q_e^2 \times t}{1 + k_a \times q_e \times t} \quad (1)$$

where q is the amount of adsorbate (mg g^{-1}) at time t (min), q_e is the amount of adsorbate at equilibrium (mg g^{-1}), and k_a (g mg^{-1} min^{-1}) is the kinetic constant for the pseudo-second order adsorption. As can be appreciated in Figure 4, a very good fitting was obtained (R^2 = 0.993), with q_e = 129 ± 2 mg g^{-1} and k_a = 0.02 ± 0.01 g mg^{-1} min^{-1}, values that are almost

https://doi.org/10.1021/acsengineeringau.4c00011
ACS Eng. Au XXXX, XXX, XXX−XXX

identical to those obtained under N_2 sparging (q_e = 123.85 mg g^{-1}, k_a = 0.017 g mg^{-1} min^{-1}) by Zhang et al.[53]

Figure 5 shows the effect of US on the decay of Cr(VI) in the presence of NSTAR and Cit (a) and EDTA (b). Four

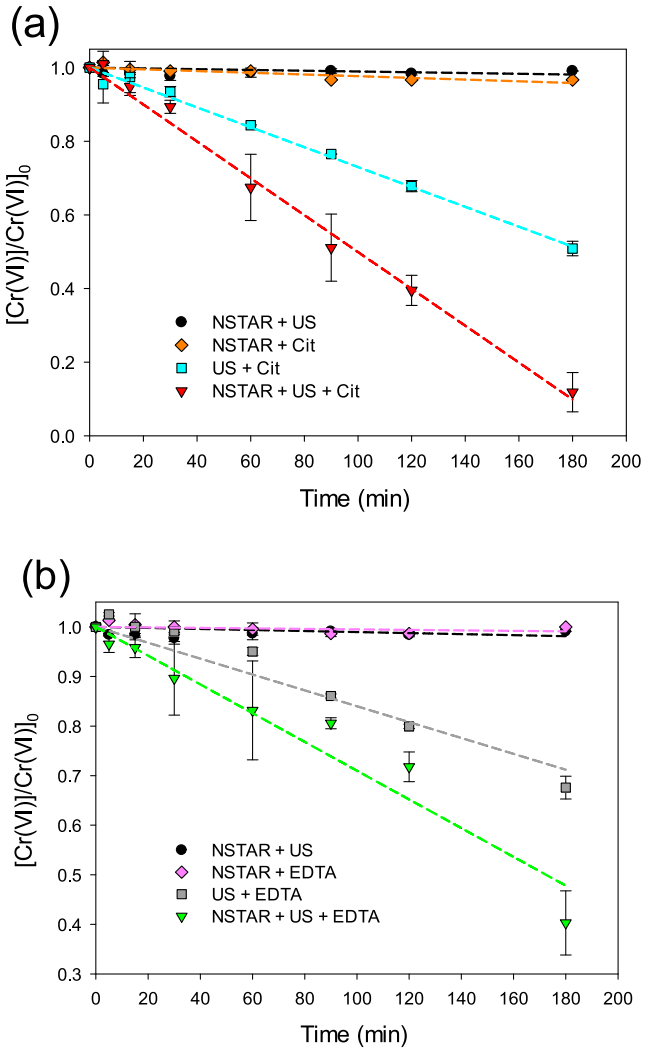

Figure 5. Temporal profiles of normalized Cr(VI) concentration ($[Cr(VI)]/[Cr(VI)]_0$) in the presence of (a) NSTAR + US, NSTAR + Cit, US + Cit, and NSTAR + US + Cit and (b) NSTAR + US, NSTAR + EDTA, US + EDTA, and NSTAR + US + EDTA. Conditions: $[Cr(VI)]_0$ = 0.3 mM, Fe_T/Cr MR 3:1, pH 3, T = 30 °C, air bubbling agitation, [Cit] = 2 mM or [EDTA] = 1 mM. Dashed lines are linear fittings.

different situations are compared: with NSTAR or CA under US, and with the combination of CA and NSTAR, with and without US.

Figure 5a shows that Cr(VI) removal is negligible when NSTAR are combined with US in the absence of Cit or when NSTAR are combined with Cit in the absence of US (less than 5% at 180 min in the last case). This effect can be attributed to the magnetite protective shield of NSTAR that prevents the corrosion of the Fe^0 core, a key step for an efficient Cr(VI) reduction. In contrast, with Cit and US, without the nanoparticles, the Cr(VI) removal attains 49%, with an 1.8-fold increase after addition of NSTAR (88%). Figure 5b indicates that, as observed with Cit, no Cr(VI) removal is obtained after combination of EDTA with NSTAR in the absence of US. In the US + EDTA system, a 32% decrease in initial Cr(VI) is obtained after 180 min; while in the ternary NSTAR + US + EDTA system, a final Cr(VI) removal of 59% is obtained, a similar 1.8-fold increase as observed for the Cit case. In contrast to prior findings at pH 2,[10] Cit is a more effective donor than EDTA at pH 3. This can be explained by the formation of complexes between the anionic Cr(VI) species and the protonated carboxylic groups of the CAs, more reactive toward reduction than bare Cr(VI).[54] Comparing the pK_as of the carboxylic groups of Cit (pK_{a1} = 3.13, pK_{a2} = 4.76, pK_{a3} = 6.40)[55] with those of EDTA (pK_{a1} = 0, pK_{a2} = 1.5, pK_{a3} = 2, pK_{a4} = 2.66),[56] it is clear that the higher pK_as of Cit facilitate the formation of these complexes.

According to Figures 4 and 5, the Cr(VI) removal by NSTAR under US in the absence of additives is negligible and contrasts with the results obtained by Zhou et al., where US significantly enhances both the reaction rate and the efficiency of Cr(VI) removal with nZVI (see Table S1 and refs 31,35). The authors indicate that US contributes to the reaction by increasing the available surface area of the nZVI particles, creating new active sites and removing reaction products that cover the nZVI surface. However, their results cannot be compared with those presented here because the authors used a different nZVI material (borohydride-synthesized and highly reactive) and experimental conditions, such as US frequency, Cr(VI) initial concentration, and Fe/Cr MR. Moreover, as shown in Table S1 and Section S3, the final Fe/reduced Cr(VI) MRs for the optimal conditions (NSTAR + US + CAs) indicate that NSTAR combined with US and CAs can be as efficient as N25, and even more reactive than nZVI synthesized using borohydride.

On the other hand, the addition of Cit and EDTA enhances the Cr(VI) removal capacity of NSTAR (Figure 5) due to the ability of CAs to complex the formed Fe(III) and Cr(III), inhibiting the formation of the Fe(III)−Cr(III) passive layer $(Cr_xFe_{1-x})(OH)_3/Cr_xFe_{1-x}OOH$ (see eqs 12 and 13 in Section 3.4).[15,18,57] As Fe(II) is generated at a low rate in solution, it reacts with Cr(VI), which explains why it was not detected in any case (Section 3.3), despite the presence of Cit was reported to enhance the recycling of Fe(II)/Fe(III) on the surface of nZVI in 2,4-dichlorophenol degradation experiments with modified nZVI.[58]

Another possibility for the enhancement of Cr(VI) reduction by nZVI in the presence of CAs has been proposed by Zhou et al.[59−61] The authors hypothesized that EDTA enhances H_2O_2 production through the reaction of eq 2, where the peroxide of the left term is generated after O_2 oxidation of the EDTA-Fe(II) complex.

$$[(EDTA)Fe^{III}(O_2^{2-})Fe^{III}(EDTA)]^{4-} \rightarrow 2[Fe^{III}(EDTA)H_2O]^- + H_2O_2 \quad (2)$$

However, as Cr(VI) removal in the NSTAR + EDTA or NSTAR + Cit systems without US was negligible (Section 3.2), this effect can be neglected, otherwise the formed H_2O_2 would contribute to Cr(VI) reduction.[10,11]

The effect of CAs was confirmed by monitoring the evolution of Fe_T concentration in solution (0.076, 0.18, and 0.26 mM after 180 min for NSTAR + US, NSTAR + US + EDTA, and NSTAR + US + Cit, respectively, Figure 6), which indicates that EDTA and Cit promote the formation of soluble Fe complexes and, more importantly, expose active sites for Cr(VI) removal on the iron nanoparticles.

https://doi.org/10.1021/acsengineeringau.4c00011
ACS Eng. Au XXXX, XXX, XXX−XXX

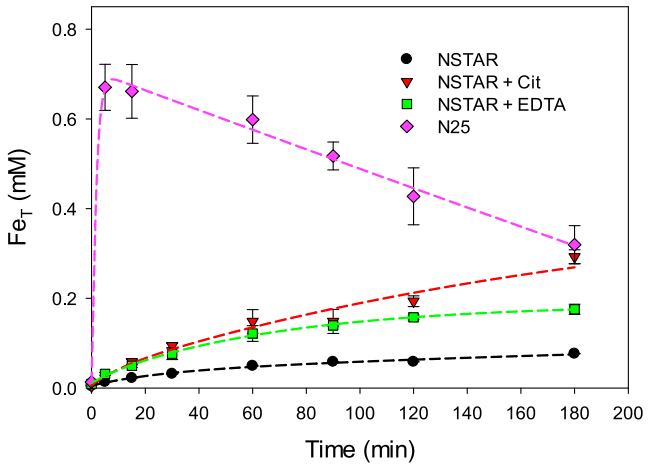

Figure 6. Temporal profiles of Fe_T concentration in the sonochemical reactor. Conditions: $[Cr(VI)]_0$ = 0.3 mM, Fe_T/Cr MR 3:1, pH 3, T = 30 °C, air bubbling, [Cit] = 2 mM, [EDTA] = 1 mM.

Figures 4 and 5 indicate that a zero-order kinetic regime is followed for Cr(VI) sonochemical removal in the presence of NSTAR and CAs. The zero-order rate constants (k_0) extracted from these figures are shown in Table 2, and a rather good

Table 2. Calculated Zero-Order Rate Constants (k_0) and R^2 Coefficients for Cr(VI) Decay under the Indicated Conditions[a]

experiment	k_0, M min^{-1} × 10^7	R^2
US + Cit	8.1 ± 0.3	0.992
NSTAR + US + Cit	15.0 ± 0.3	0.992
US + EDTA	4.8 ± 0.4	0.976
NSTAR + US + EDTA	8.7 ± 0.6	0.943

[a]Data Extracted from Linear Fittings in Figures 4 and 5.

fitting ($R^2 \geq 0.94$) was observed. Other conditions (NSTAR + US, NSTAR + Cit, and NSTAR + EDTA) did not follow this zero-order regime and are not included in Table 2.

This zero-order kinetic regime was previously observed by our group in the US + CAs system (no nZVI),[10,11] although the reaction rates were higher than those reported here, which can be explained by the lower pH (2), higher power input, and a different reactor setup. The only kinetic model reported in the literature for Cr(VI) removal with nZVI under US (no CAs) is a two-parameter pseudo-first-order model proposed by Zhou et al.,[31] although the authors used a different nZVI material (prepared from sodium borohydride).

In the SI, Section S3, Table S1 shows the Cr(VI) removal capacity of NSTAR under different conditions obtained in the present work compared with other reported studies of Cr(VI) removal with nZVI. The results indicate that the combinations NSTAR + CAs + US were among the most efficient nZVI systems considering the lower final Fe_T/Cr(VI) MR and reaction times for aqueous Cr(VI) treatment. The use of CAs represents a very efficient way for NSTAR use compared with activation strategies such as time, electromagnetic, or heating. Regarding the reaction times, it is important to highlight that only 3 h were needed to achieve 89% Cr(VI) removal when using Cit, while, in other cases, days were necessary. Working pH is also a key parameter, as the most efficient results have been obtained at pH 3.

3.3. Iron in Solution

Figure 6 shows the temporal profiles of Fe_T concentration in the aqueous phase inside the sonochemical reactor determined after centrifugation of the nanoparticles.

A continuous increase in iron concentration with time can be observed in the experiments with NSTAR and US, either with or without CAs. In the case of NSTAR alone, the final Fe_T was 0.076 mM, while it was 0.29 mM and 0.16 mM for the systems with Cit and EDTA, respectively, indicating that both CAs enhance Fe leaching. As Cr(VI) reduction was almost negligible in the absence of CAs, it can be assumed that Fe is leached to the solution as Fe^{2+} from the NSTAR shell, and/or that Fe^0 and Fe^{2+} were consumed by an undesired reaction (e.g., by oxidation by HO$^\bullet$ or H_2O_2 generated during the sonolytic treatment).[11,30] The addition of CAs enhanced the removal of the NSTAR passivation layer,[52] leaving exposed active sites on the nZVI surface that can promote Cr(VI) reduction. Figure 6 also indicates that when N25 was used under US, the Fe_T concentration reached a maximum of 0.67 mM (75% of the total Fe added) at 5 min, followed by a continuous decrease up to a final value of 0.32 mM at 180 min. This decrease is caused by the partial precipitation of Fe(III) as oxo-hydroxides, which were actually observed as a brown solid settled on the bottom of the reactor. A similar trend was reported by other authors, although the higher percentage of maximum Fe_T found (cf. 75% vs 40%[18] and 0.6%)[53] reflects the impact of US. Therefore, the considerable reactivity of N25 nanoparticles also implied a higher iron dissolution rate and a higher final Fe_T. As iron should be removed before disposal of the treated solution, a lower final Fe_T implies a lower dose of chemical additives and of sludge generation, being another advantage of the use of the NSTAR + CAs system over N25.

Contrarily to the results obtained in previous works,[18,53] Fe(II) was never found during the experiments, probably due to (1) the low Fe(II) generation rate in the experiments with NSTAR; (2) its fast oxidation by Cr(VI) ($k_2 \approx 1200$ M^{-1} s^{-1}, calculated from[62] at pH 3 and 25 °C); (3) Fe(II) oxidation by reactive species generated under water sonolysis, such as HO$^\bullet$ ($k_2 = 4.3 \times 10^8$ M^{-1} s^{-1}) and H_2O_2 ($k_2 = 43$ M^{-1} s^{-1});[63] or (4) Fe(II) precipitation as $FeCr_2O_4$ with the generated Cr(III), as detected by XRD by Zhou et al.[31]

3.4. Postulated Mechanisms

Several pathways can be proposed for the mechanism of Cr(VI) removal in the present conditions: (I) reduction by H_2O_2, produced either by Fe^0 corrosion or H_2O sonolysis; (II) reduction by organic radicals generated after Cit or EDTA reaction with oxidative species generated by US; (III) direct reduction by nZVI; and (IV) reduction by Fe(II) generated after nZVI corrosion or Fe(III) reduction by H_2O_2 or organic radicals in Fenton-like processes. These different pathways are discussed below.

Reduction by H_2O_2 produced by Fe^0 corrosion or H_2O sonolysis (pathway I, eq 3) was indicated as the main reaction for Cr(VI) reduction under US.[10,11] The homogeneous chemistry between Cr(VI) and H_2O_2 in water is complex and involves different reactions and the formation of several Cr(V) and Cr(IV) species until reduction to Cr(III), the nontoxic final product that under acidic conditions can be described by the stoichiometry proposed by eq 3.[10,11,64,65]

https://doi.org/10.1021/acsengineeringau.4c00011
ACS Eng. Au XXXX, XXX, XXX−XXX

$$2HCrO_4^- + (3 + 2n)H_2O_2 + 8H^+ \rightarrow 2Cr^{3+} + (8 + 2n)H_2O + (3 + n)O_2 \quad (3)$$

where n accounts for H_2O_2 consumption related with $(CrO(O_2)_2)$ disproportionation to Cr(VI), being $n = 0$ the simplest case.[66]

Cr(VI) reduction under US in the presence of CAs (no Fe nanoparticles, pathway II) has been postulated to occur through reaction with H_2O_2 (eq 3), $HO_2^\bullet$ (eq 4) or with reducing $R^\bullet$ and $ROO^\bullet$ radicals derived from EDTA or Cit (eqs 5 and 6). This pathway can lead to Cr(V), Cr(IV), and Cr(III).[10,11] Cr(V)/(IV)/(III) reoxidation to Cr(VI) by $HO^\bullet$ (eq 7) cannot be ruled out as this radical is generated in the primary process of the sonolytic water decomposition described in the SI, Section S1. However, this reaction is inhibited in the presence of CAs because the attack to the organic compound is preferred as it is present at relatively high concentration. In fact, several years ago it was shown that Cr(III)−EDTA complexes reoxidize very slowly to Cr(VI) under US.[67]

$$Cr(VI)/(V)/(IV) + HO_2^\bullet \rightarrow Cr(V)/(IV)/(III) + H^+ + O_2 \quad (4)$$

$$Cr(VI)/(V)/(IV) + R^\bullet \rightarrow Cr(V)/(IV)/(III) + R_{ox} \quad (5)$$

$$Cr(VI)/(V)/(IV) + ROO^\bullet \rightarrow Cr(V)/(IV)/(III) + R_{ox} \quad (6)$$

$$Cr(V)/(IV)/(III) + HO^\bullet \rightarrow Cr(VI)/(V)/(IV) + HO^- \quad (7)$$

$$Cr(V) + H_2O_2 \rightarrow Cr(VI) + HO^\bullet + OH^- \quad (8)$$

Although the intermediate peroxyl species produced by reaction of eq (S11) can scavenge the reducing radicals $R^\bullet$ when O_2 is present, it can still be expected to reduce Cr(VI) by eq 6. H_2O_2 could also oxidize Cr(V) (eq 8); this reaction produces $HO^\bullet$ and a Fenton-type reaction, leading to Cr(VI) regeneration.[68,69] In addition, EDTA and Cit (and their degradation products) can stabilize intermediate Cr(V) compounds, enhancing their direct transformation into different Cr(III) species.[10,11] Moreover, CAs act as Cr(IV) reductants (according to the high redox potential of the Cr(IV)/Cr(III) couple, $E^0 = 2.1$ V[9]).

The mechanism of Cr(VI) removal by nZVI (in the absence of CAs and US, pathway (III)) may comprise three distinct processes according to recent works:[23,53,70] (1) Cr(VI) adsorption onto the external nZVI surface, (2) Cr(VI) reduction to Cr(III), facilitated by the transfer of electrons from nZVI and/or Fe(II) species, and (3) mass transport processes resulting in the precipitation or coprecipitation of Cr(III) and Fe(III) hydroxides. Although the detailed mechanism is still controversial, it is generally accepted that Cr(VI) is reduced to Cr(III); and correspondingly, Fe^0 is oxidized to Fe^{2+} (eq 9) and/or Fe^{3+} (eq 10), although the Fe^{2+} generated in eq 9 would be rapidly oxidized to Fe(III) by Cr(VI) (eq 11 and pathway (IV)).[7,23,25,53] Indeed, at 180 min of reaction, almost identical Cr(VI) removals (0.26 and 0.18 mM for Cit and EDTA, respectively, Figure 4) and Fe_T in solution (0.29 and 0.16 mM for Cit and EDTA, respectively, Figure 6) were obtained for the experiments with NSTAR and CAs under US, reflecting an 1:1 Cr(VI)/Fe^0 molar ratio. This is indicative that eq 10 is more representative of the system stoichiometry than eq 9, and that Fe^0 oxidation to Fe(III) is the main step of the Cr(VI) removal mechanism. However, the experimental result 1:1 Cr(VI)/Fe^0 molar ratio can be due to eq 10 or to the sum of eqs 9 and 11, which represents the contribution of both pathways (III) and (IV). Once formed, Cr(III) would remain in solution[13,15,18,31,48] and/or be immobilized through precipitation/incorporation on the nZVI surface, forming alloy-like Cr−Fe hydroxides, as represented by eqs 12 and 13,[7,14,18,20,23,25,53,71] with x being approximately 0.667.[71]

$$2HCrO_4^- + 14H^+ + 3Fe^0(s) \rightarrow 2Cr^{3+} + 8H_2O + 3Fe^{2+} \quad (9)$$

$$HCrO_4^- + 7H^+ + Fe^0(s) \rightarrow Cr^{3+} + 4H_2O + Fe^{3+} \quad (10)$$

$$HCrO_4^- + 7H^+ + 3Fe^{2+} \rightarrow Cr^{3+} + 4H_2O + 3Fe^{3+} \quad (11)$$

$$xCr^{3+} + (1 - x)Fe^{3+} + 3H_2O \rightarrow (Cr_xFe_{1-x})(OH)_3 + 3H^+ \quad (12)$$

$$xCr^{3+} + (1 - x)Fe^{3+} + 2H_2O \rightarrow Cr_xFe_{1-x}OOH + 3H^+ \quad (13)$$

In particular, when US[15] or CAs[52] were used in combination with nZVI for Cr(VI) reduction, most of the formed Cr(III) remained in solution, reducing the contribution of eqs 12 and 13 to nZVI passivation. Although Zhou et al. (2015)[31] and (2016)[35] reported that only ≈20% of the formed remained in solution after nZVI + US treatment of Cr(VI), their final solution pH was neutral, favoring Cr(III) precipitation; while in our case, the initial pH 3 was constant, reducing the influence of these reactions.

Regarding the participation of Fenton-like reactions (involving surface or dissolved iron species and H_2O_2) in pathway (IV), the mechanism is still under intense and controversial discussion in the literature and can be found elsewhere.[28,63,72−74] There is consensus around iron cycling between Fe(II) and Fe(III) with $HO^\bullet$ generation. A similar mechanism occurs when dissolved iron is replaced by iron nanoparticles,[17,72,74] as Fe^0 is oxidized to Fe(II) leading to Fenton reactions. However, as in the present work, Fe(II) was not detected in solution, the role of Fenton processes may be considered negligible. Besides, as stated above, the $HO^\bullet$ formed would be scavenged by CAs, generating organic reducing radicals that contribute to Cr(VI) removal (eqs 5 and 6).

When comparing the CAs, the present work shows that Cit is more efficient than EDTA for Cr(VI) removal by NSTAR under US. Cit not only exhibits a higher Cr(VI) reduction rate but also the Cr(III)-Cit complex is oxidized to Cr(VI) by H_2O_2 300 times slower than Cr(III)-EDTA,[75] rendering less probable its reoxidation to the toxic Cr(VI) if accidentally discarded in the environment. Additionally, Cit is a natural biodegradable ligand and, thus, less environmentally harmful than EDTA,[76] which is a nonbiodegradable synthetic chelator, and its degradation intermediates could pollute water resources.

NSTAR can be promoted for in situ injection in polluted aquifers and the process might be scaled up. For this, two alternatives of the combined NSTAR + US + Cit process can be proposed: (1) An NSTAR activation treatment faster (3 h)

https://doi.org/10.1021/acsengineeringau.4c00011
ACS Eng. Au XXXX, XXX, XXX−XXX

than the one suggested by the producer company (24−48 h), where NSTAR particles are suspended in an aqueous Cit solution and then irradiated with US, followed by injection of the activated NSTAR + Cit suspension; (2) Injection of the suspension of not activated NSTAR + Cit, followed by in situ application of US. Both procedures have been tested for soil remediation, but the treatment has still to be improved.[77,78]

4. CONCLUSIONS

The removal of Cr(VI) was efficient when the combination of commercial air-stable nZVI NSTAR powder, CAs as EDTA or Cit and US, was applied and greatly enhanced compared with the use of these processes alone.

No Cr(VI) decay up to 180 min was observed when NSTAR, NSTAR + US, or NSTAR + CAs systems were used, while the US + EDTA and US + Cit systems (without NSTAR) displayed a 32 and 49% of Cr(VI) removal, respectively. However, the ternary NSTAR + US + EDTA and NSTAR + US + Cit systems reached 59 and 88% of Cr(VI) removal at 180 min, reflecting a clear synergy in these ternary systems. A linear Cr(VI) decay was observed for both Cit and EDTA experiments, and zero-order rate constants were calculated. Although commercial N25 combined with US showed a higher Cr(VI) initial removal rate than the NSTAR + CAs + US systems, the final Cr(VI) removal was lower, with a higher amount of total iron in solution.

Both CAs and US were necessary for an efficient Cr(VI) reduction when using NSTAR (not activated) because of the ability of the combination to remove the passive layer of iron oxides. This allows the use of the commercial powder with no further time-consuming activation steps. Besides, CAs may play a role on Cr(VI) reduction by stabilizing intermediate Cr(V) compounds, enhancing their direct transformation into different Cr(III) species. Cit was found to be a better additive because it can strongly complex Cr(V) and Cr(III) species and it is a safe nontoxic compound.

■ ASSOCIATED CONTENT

Supporting Information

The Supporting Information is available free of charge at https://pubs.acs.org/doi/10.1021/acsengineeringau.4c00011.

Simplified set of reactions in sonochemical aqueous systems; sonochemical reaction setup; comparison of Cr(VI) removal capacity of NSTAR with other nZVI materials under different conditions (PDF)

■ AUTHOR INFORMATION

Corresponding Author

Marta I. Litter − *IIIA (CONICET-UNSAM), Instituto de Investigación e Ingeniería Ambiental, Escuela de Hábitat y Sostenibilidad, Universidad Nacional de General San Martín, 1650 San Martín, Prov. de Buenos Aires, Argentina;* orcid.org/0000-0002-0312-0177; Email: martalitter24@gmail.com

Authors

Lucia Cancelada − *Gerencia Química, Comisión Nacional de Energía Atómica-CONICET, 1650 San Martín, Prov. de Buenos Aires, Argentina; Energy Technologies Area, Lawrence Berkeley National Laboratory, Berkeley, California 94720, United States;* Present Address: Department of Chemistry and Biochemistry, University of California San Diego, 9500 Gilman Drive, La Jolla, California 92093, United States

Jorge M. Meichtry − *Gerencia Química, Comisión Nacional de Energía Atómica-CONICET, 1650 San Martín, Prov. de Buenos Aires, Argentina; Centro de Tecnologías Químicas, Facultad Regional Buenos Aires, Universidad Tecnológica Nacional, C1179AAQ Ciudad Autónoma de Buenos Aires, Argentina;* orcid.org/0000-0002-4832-7956

Hugo Destaillats − *Energy Technologies Area, Lawrence Berkeley National Laboratory, Berkeley, California 94720, United States;* orcid.org/0000-0002-2132-3816

Complete contact information is available at: https://pubs.acs.org/10.1021/acsengineeringau.4c00011

Author Contributions

L.C.: methodology, investigation, formal analysis, original draft preparation, review and editing. J.M.M.: methodology, investigation, formal analysis, original draft preparation, review and editing. H.D.: review and editing, supervision, resources. M.I.L.: conceptualization, methodology, review and editing, supervision, resources, funding acquisition, and project administration. CRediT: **Lucia Cancelada** formal analysis, investigation, methodology, writing-original draft, writing-review & editing; **Jorge Martín Meichtry** formal analysis, investigation, methodology, writing-original draft, writing-review & editing; **Hugo Destaillats** supervision, writing-review & editing; **Marta I. Litter** methodology, project administration, resources, supervision, writing-review & editing.

Notes

The authors declare no competing financial interest.

■ ACKNOWLEDGMENTS

This work was supported by the Agencia Nacional de Promoción Científica y Tecnológica (ANPCyT) from Argentina under PICT-2015-0208. The authors are grateful to Dr. Emilia Halac for Raman measurements, to Dr. Cinthia Ramos for Mössbauer measurements and interpretation, to Cristian Oubiña for DRX measurements (Dr. Vega's laboratory), and to Natalia Grillo for BET measurements, all of them from Comisión Nacional de Energía Atómica (Argentina).

■ REFERENCES

(1) Tumolo, M.; Ancona, V.; De Paola, D.; Losacco, D.; Campanale, C.; Massarelli, C.; Uricchio, V. F. Chromium Pollution in European Water, Sources, Health Risk, and Remediation Strategies: An Overview. *Int. J. Environ. Res. Public Health* **2020**, *17*, 5438.

(2) Itankar, N.; Patil, Y. Assessing Physicochemical Technologies for Removing Hexavalent Chromium from Contaminated Waters—An Overview and Future Research Directions. *Water, Air, Soil Pollut.* **2022**, *233*, 355.

(3) Liang, J.; Huang, X.; Yan, J.; Li, Y.; Zhao, Z.; Liu, Y.; Ye, J.; Wei, Y. A review of the formation of Cr(VI) via Cr(III) oxidation in soils and groundwater. *Sci. Total Environ.* **2021**, *774*, No. 145762.

(4) Litter, M. I. Last advances on TiO_2-photocatalytic removal of chromium, uranium and arsenic. *Curr. Opin. Green Sustainable Chem.* **2017**, *6*, 150−158.

(5) World Health Organization. Guidelines for Drinking-Water Quality, 4th ed.; WHO Chronicle, 2011.

(6) Brown, E. G.; Alexeeff, G. V. Public Health Goals for Chemicals in Drinking Water. https://oehha.ca.gov/media/downloads/water/chemicals/phg/cr6phg072911.pdf. (access on August 31, 2023).

(7) Yang, W.; Chai, L.; Yang, Z.; Zhao, F.; Liao, Q.; Si, M. Mechanism of Chemical Reduction of Cr(VI). In *Remediation of Chromium-Contaminated Soil: Theory and Practice*; Springer Nature Singapore: Singapore, 2023; pp 171−255 978-981-99-5463-6.
(8) Xing, X.; Alharbi, N. S.; Ren, X.; Chen, C. A comprehensive review on emerging natural and tailored materials for chromium-contaminated water treatment and environmental remediation. *J. Environ. Chem. Eng.* **2022**, *10*, No. 107325.
(9) Litter, M. I.; Quici, N.; Meichtry, J. M.; Senn, A. M. Photocatalytic Removal of Metallic and Other Inorganic Pollutants. In *Photocatalysis: Applications*; Dionysiou, D. D.; Li Puma, G.; Ye, J.; Schneider, J.; Bahnemann, D., Eds.; Royal Society, Chapter 2, 2016; pp 35−71 9781782620419.
(10) Meichtry, J. M.; Slodowicz, M.; Cancelada, L.; Destaillats, H.; Litter, M. I. Sonochemical reduction of Cr(VI) in air in the presence of organic additives: what are the involved mechanistic pathways? *Ultrason. Sonochem.* **2018**, *48*, 110−117.
(11) Meichtry, J. M.; Cancelada, L.; Destaillats, H.; Litter, M. I. Effect of different gases on the sonochemical Cr(VI) reduction in the presence of citric acid. *Chemosphere* **2020**, *260*, No. 127211.
(12) Xu, M.; Wu, C.; Zhou, Y. Advancements in the Fenton Process for Wastewater Treatment. In *Advanced Oxidation Processes − Applications, Trends and Prospects*; Bustillo-Lecompte, C., Ed.; IntechOpen, 2020; pp 61−77.
(13) Parnis, M.; García, F. E.; Toledo, M. V.; Montesinos, V. N.; Quici, N. Zerovalent Iron Nanoparticles-Alginate Nanocomposites for Cr(VI) Removal in Water—Influence of Temperature, pH, Dissolved Oxygen, Matrix, and nZVI Surface Composition. *Water* **2022**, *14*, 484.
(14) Song, H.; Liu, W.; Meng, F.; Yang, Q.; Guo, N. Efficient Sequestration of Hexavalent Chromium by Graphene-Based Nanoscale Zero-Valent Iron Composite Coupled with Ultrasonic Pretreatment. *Int. J. Environ. Res. Public Health* **2021**, *18*, 5921.
(15) Diao, Z.-H.; Yan, L.; Dong, F.-X.; Chen, Z.-L.; Guo, P.-R.; Qian, W.; Zhang, W.-X.; Liang, J.-Y.; Huang, S.-T.; Chu, W. Ultrasound-assisted catalytic reduction of Cr(VI) by an acid mine drainage based nZVI coupling with FeS_2 system from aqueous solutions: Performance and mechanism. *J. Environ. Manage.* **2021**, *278*, No. 111518.
(16) Lan, L. E.; Reina, F. D.; De Seta, G. E.; Meichtry, J. M.; Litter, M. I. Comparison between different technologies (zerovalent iron, coagulation-flocculation, adsorption) for arsenic treatment at high concentrations. *Water* **2023**, *15*, 1481.
(17) *Iron Nanomaterials for Water and Soil Treatment*, 1st ed.; Litter, M. I.; Quici, N.; Meichtry, M., Eds.; CRC Press: New York, 2018. https://www.routledge.com/Iron-Nanomaterials-for-Water-and-Soil-Treatment/Litter-Quici-Meichtry/p/book/9789814774673.
(18) Montesinos, V. N.; Quici, N.; Halac, B. E.; Leyva, A. G.; Custo, G.; Bengio, S.; Zampieri, G.; Litter, M. I. Highly efficient removal of Cr(VI) from water with nanoparticulated zerovalent iron: Understanding the Fe(III)-Cr(III) passive outer layer structure. *Chem. Eng. J.* **2014**, *244*, 569−575.
(19) Li, K.; Li, J.; Qin, F.; Dong, H.; Wang, W.; Luo, H.; Qin, D.; Zhang, C.; Tan, H. Nano zero valent iron in the 21st century: A data-driven visualization and analysis of research topics and trends. *J. Cleaner Prod.* **2023**, *415*, No. 137812.
(20) Huang, X.-y.; Ling, L.; Zhang, W.-x. Nanoencapsulation of hexavalent chromium with nanoscale zero-valent iron: High resolution chemical mapping of the passivation layer. *J. Environ. Sci.* **2018**, *67*, 4−13.
(21) Calderon, B.; Fullana, A. Heavy metal release due to aging effect during zero valent iron nanoparticles remediation. *Water Res.* **2015**, *83*, 1−9.
(22) Montesinos, V. N.; Quici, N.; Litter, M. I. Visible light enhanced Cr(VI) removal from aqueous solution by nanoparticulated zerovalent iron. *Catal. Commun.* **2014**, *46*, 57−60.
(23) Xing, X.; Ren, X.; Alharbi, N. S.; Chen, C. Efficient adsorption and reduction of Cr(VI) from aqueous solution by Santa Barbara Amorphous-15 (SBA-15) supported Fe/Ni bimetallic nanoparticles. *J. Colloid Interface Sci.* **2023**, *629*, 744−754.
(24) NANOFERSTAR https://nanoiron.cz/en/products/zero-valent-iron-nanoparticles/nanofer-star. (access on Feb 14, 2024).
(25) Ribas, D.; Černík, M.; Benito, J. A.; Filip, J.; Marti, V. Activation process of air stable nanoscale zero-valent iron particles. *Chem. Eng. J.* **2017**, *320*, 290−299.
(26) Víchová, V.; Oborná, J.; Jakubec, P.; Filip, J. Activation of air-stable zero-valent iron nanoparticles: comparison of different approaches. *Proceedings of the 12th International Conference on Nanomaterials*; Brno, Czech Republic, October 21−23, 2020, DOI: 10.37904/nanocon.2020.3721.
(27) Adewuyi, Y. G. Sonochemistry: Environmental Science and Engineering Applications. *Ind. Eng. Chem. Res.* **2001**, *40*, 4681−4715.
(28) Litter, M. I. Introduction to Oxidative Technologies of Water Treatment. In *Advanced Nano-Bio Technologies for Water and Soil Treatment*; Filip, J.; Cajthaml, T.; Najmanová, P.; Černík, M.; Zbořil, R., Eds.; Springer, 2020; pp 119−175 978-3-030-29839-5.
(29) Hung, H. M.; Hoffmann, M. R. Kinetics and Mechanism of the Enhanced Reductive Degradation of CCl_4 by Elemental Iron in the Presence of Ultrasound. *Environ. Sci. Technol.* **1998**, *32* (32), 3011−3016.
(30) Ma, Y.-S. Short review: Current trends and future challenges in the application of sono-Fenton oxidation for wastewater treatment. *Sustainable Environ. Res.* **2012**, *22*, 271−278.
(31) Zhou, X.; Lv, B.; Zhou, Z.; Li, W.; Jing, G. Evaluation of highly active nanoscale zero-valent iron coupled with ultrasound for chromium(VI) removal. *Chem. Eng. J.* **2015**, *281*, 155−163.
(32) Zhang, W. H.; Quan, X.; Wang, J. X.; Zhang, Z. Y.; Chen, S. Rapid and complete dechlorination of PCP in aqueous solution using Ni-Fe nanoparticles under assistance of ultrasound. *Chemosphere* **2006**, *65*, 58−64.
(33) Taha, M. R.; Ibrahim, A. H. Characterization of nano zero-valent iron (nZVI) and its application in sono-Fenton process to remove COD in palm oil mill effluent. *J. Environ. Chem. Eng.* **2014**, *2*, 1−8.
(34) Sadjadi, S. *Nanomaterials for Environmental Protection*; Kharisov, B. I.; Kharissova, O. V.; Rasika Dias, H. V., Eds.; John Wiley & Sons: Hoboken, 2014; pp 403−427.
(35) Zhou, X.; Jing, G.; Lv, B.; Zhou, Z.; Zhu, R. Highly efficient removal of chromium(VI) by Fe/Ni bimetallic nanoparticles in an ultrasound-assisted system. *Chemosphere* **2016**, *160*, 332−341.
(36) Jin, X.; Zhuang, Z.; Yu, B.; Chen, Z.; Chen, Z. Functional chitosan-stabilized nanoscale zero-valent iron used to remove acid fuchsine with the assistance of ultrasound. *Carbohydr. Polym.* **2016**, *136*, 1085−1090.
(37) Bounab, N.; Duclaux, L.; Reinert, L.; Oumedjbeur, A.; Boukhalfa, C.; Penhoud, P.; Muller, F. Improvement of zero valent iron nanoparticles by ultrasound-assisted synthesis, study of Cr(VI) removal and application for the treatment of metal surface processing wastewater. *J. Environ. Chem. Eng.* **2021**, *9*, No. 104773.
(38) Nanofer25 https://nanoiron.cz/en/products/zero-valent-iron-nanoparticles/nanofer-25. (access on Feb 14, 2024).
(39) NANOFER-STAR-processing-activation-manual. https://nanoiron.cz/getattachment/7aa3e8c5-5701-4a47-b05c-b91f87279aae/NANOFER-STAR-processing-activation-manual.aspx. (access on Jan 13, 2024).
(40) Kašlík, J.; Kolařík, J.; Filip, J.; Medřík, I.; Tomanec, O.; Petr, M.; Malina, O.; Zbořil, R.; Tratnyek, P. G. Nanoarchitecture of advanced core-shell zero-valent iron particles with controlled reactivity for contaminant removal. *Chem. Eng. J.* **2018**, *354*, 335−345.
(41) Oprčkal, P.; Mladenovič, A.; Vidmar, J.; Pranjić, A. M.; Milačič, R.; Ščančar, J. Critical evaluation of the use of different nanoscale zero-valent iron particles for the treatment of effluent water from a small biological wastewater treatment plant. *Chem. Eng. J.* **2017**, *321*, 20−30.
(42) Liu, Y.; Majetich, S. A.; Tilton, R. D.; Sholl, D. S.; Lowry, G. V. TCE Dechlorination Rates, Pathways, and Efficiency of Nanoscale Iron Particles with Different Properties. *Environ. Sci. Technol.* **2005**, *39*, 1338−1345.

https://doi.org/10.1021/acsengineeringau.4c00011
ACS Eng. Au XXXX, XXX, XXX−XXX

(43) Nikitenko, S. I.; Le Naour, C.; Moisy, P. Comparative study of sonochemical reactors with different geometry using thermal and chemical probes. *Ultrason. Sonochem.* **2007**, *14*, 330−336.
(44) Iida, Y.; Yasui, K.; Tuziuti, T.; Sivakumar, M. Sonochemistry and its dosimetry. *Microchem. J.* **2005**, *80*, 159−164.
(45) ASTM. D1687−92 Standard Test Methods for Chromium in Water. 1996 DOI: 10.1520/D1687-92R96.
(46) Sandell, E. B. *Colorimetric Determination of Traces of Metals*; Interscience Publishers Inc: New York, 1959.
(47) NANO IRON. NANOFER STAR (NSTAR) Safety Data Sheet (According to Regulation EC No. 1907/2006). https://nanoiron.cz/getattachment/81874e2a-f96f-455e-8551-14f40f67868c/NANOFER-STAR-SDS-English.aspx. (access on Jan 13, 2024).
(48) Sciscenko, I.; Luca, V.; Ramos, C. P.; Scott, T. B.; Montesinos, V. N.; Quici, N. Immobilization of nanoscale zerovalent iron in hierarchically channelled polyacrylonitrile for Cr(VI) remediation in wastewater. *J. Water Process Eng.* **2021**, *39*, No. 101704.
(49) WinNormos-for-Igor Software Package. http://www.wissel-gmbh.de/index.php?option=com_content&task=view&id=55&Itemid=116. (access on Jan 17, 2024).
(50) Meichtry, J. M.; Brusa, M.; Mailhot, G.; Grela, M. A.; Litter, M. I. Heterogeneous photocatalysis of Cr(VI) in the presence of citric acid over TiO_2 particles: Relevance of Cr(V)-citrate complexes. *Appl. Catal., B* **2007**, *71*, 101−107.
(51) García, F. E.; Plaza-Cazón, J.; Montesinos, V. N.; Donati, E. R.; Litter, M. I. Combined strategy for removal of Reactive Black 5 by biomass sorption on Macrocystis pyrifera and zerovalent iron nanoparticles. *J. Environ. Manage.* **2018**, *207*, 70−79.
(52) Zhou, H.; Ye, M.; Zhao, Y.; Baig, S. A.; Huang, N.; Ma, M. Sodium citrate and biochar synergistic improvement of nanoscale zero-valent iron composite for the removal of chromium (VI) in aqueous solutions. *J. Environ. Sci.* **2022**, *115*, 227−239.
(53) Zhang, S.-H.; Wu, M.-F.; Tang, T.-T.; Xing, Q.-J.; Peng, C.-Q.; Li, F.; Liu, H.; Luo, X.-B.; Zou, J.-P.; Min, X.-B.; Luo, J.-M. Mechanism investigation of anoxic Cr(VI) removal by nano zero-valent iron based on XPS analysis in time scale. *Chem. Eng. J.* **2018**, *335*, 945−953.
(54) Uma, P.; Kanta Rao, P.; Sastry, M. N. Kinetics of EDTA catalyzed oxidation of I− by Cr(VI). *React. Kinet. Catal. Lett.* **1989**, *39*, 255−260.
(55) Silva, A. M. N.; Kong, X.; Hider, R. C. Determination of the pKa value of the hydroxyl group in the α-hydroxycarboxylates citrate, malate and lactate by ^{13}C NMR: implications for metal coordination in biological systems. *BioMetals* **2009**, *22*, 771−778.
(56) Ezzeddine, Z.; Batonneau-Gener, I.; Pouilloux, Y.; Hamad, H.; Saad, Z.; Kazpard, V. Divalent heavy metals adsorption onto different types of EDTA-modified mesoporous materials: Effectiveness and complexation rate. *Microporous Mesoporous Mater.* **2015**, *212*, 125−136.
(57) Petala, E.; Filip, J.; Zboril, R. Effervescent Zero-Valent Iron Compositions and Method of Remediation of Pollutants from Aqueous Solutions, International Application Published Under the Patent Cooperation Treaty (PCT). WO153,389A1, 2018.
(58) Zhang, C.; Wang, D.; Liu, Q.; Tang, J. Ligand-citric acid enhanced in-situ ROS generation by GBC@nZVI to promote the aerobic degradation of adsorbed 2,4-dichlorophenol. *Chem. Eng. J.* **2023**, *477*, No. 147126.
(59) Zhou, T.; Li, Y.; Wong, F.-S.; Lu, X. Enhanced degradation of 2,4-dichlorophenol by ultrasound in a new Fenton like system (Fe/EDTA) at ambient circumstance. *Ultrason. Sonochem.* **2008**, *15*, 782−790.
(60) Zhou, T.; Lim, T.-T.; Lu, X.; Li, Y.; Wong, F.-S. Simultaneous degradation of 4CP and EDTA in a heterogeneous Ultrasound/Fenton like system at ambient circumstance. *Sep. Purif. Technol.* **2009**, *68*, 367−374.
(61) Zhou, T.; Lim, T.-T.; Li, Y.; Lu, X.; Wong, F.-S. The role and fate of EDTA in ultrasound-enhanced zero-valent iron/air system. *Chemosphere* **2010**, *78*, 576−582.
(62) Pettine, M.; D'Ottone, L.; Campanella, L.; Millero, F. J.; Passino, R. The reduction of chromium (VI) by iron (II) in aqueous solutions. *Geochim. Cosmochim. Acta* **1998**, *62*, 1509−1519.
(63) Koppenol, W. H. Ferryl for real. The Fenton reaction near neutral pH. *Dalton Trans.* **2022**, *51*, 17496−17502.
(64) Pettine, M.; Campanella, L.; Millero, F. J. Reduction of Hexavalent Chromium by H_2O_2 in Acidic Solutions. *Environ. Sci. Technol.* **2002**, *36*, 901−907.
(65) van Niekerk, W.; Pienaar, J. J.; Lachmann, G.; van Eldik, R.; Hamza, M. A kinetic and mechanistic study of the chromium (VI) reduction by hydrogen peroxide in acidic aqueous solutions. *Water SA* **2019**, *33*, 619−625.
(66) Vander Griend, D. A.; Golden, J. S.; Arrington, C. A., Jr. Kinetics and mechanism of chromate reduction with hydrogen peroxide in base. *Inorg. Chem.* **2002**, *41*, 7042−7048.
(67) Frim, J. A.; Rathman, J. F.; Weavers, L. K. Sonochemical destruction of free and metal-binding ethylenediaminetetraacetic acid. *Water Res.* **2003**, *37*, 3155−3163.
(68) Bokare, A. D.; Choi, W. Chromate-Induced Activation of Hydrogen Peroxide for Oxidative Degradation of Aqueous Organic Pollutants. *Environ. Sci. Technol.* **2010**, *44*, 7232−7237.
(69) Bokare, A. D.; Choi, W. Advanced Oxidation Process Based on the Cr(III)/Cr(VI) Redox Cycle. *Environ. Sci. Technol.* **2011**, *45*, 9332−9338.
(70) Du, W.; Zhang, Y.; Li, Y.; Ma, X.; Zhao, C. A model for the removal of Cr(VI) in water by nanoscale zero-valent iron: quantifying the reaction process and calculating the electron efficiency. *J. Nanopart. Res.* **2023**, *25*, 119.
(71) Li, X.-q.; Cao, J.; Zhang, W.-x. Stoichiometry of Cr(VI) Immobilization Using Nanoscale Zerovalent Iron (nZVI): A Study with High-Resolution X-Ray Photoelectron Spectroscopy (HR-XPS). *Ind. Eng. Chem. Res.* **2008**, *47*, 2131−2139.
(72) Litter, M. I.; Slodowicz, M. An Overview on Heterogeneous Fenton and PhotoFenton Reactions using Zerovalent Iron Materials. *J. Adv. Oxid. Technol.* **2017**, *20*, 2371−1175.
(73) Xu, M.; Wu, C.; Zhou, Y. Advancements in the Fenton Process for Wastewater Treatment. In *Advanced Oxidation Processes − Applications, Trends and Prospects*; Bustillo-Lecompte, C., Ed.; IntechOpen, 2020; pp 61−77.
(74) Duca, C.; Bogo, H.; Litter, M. I.; San Román, E. Heterogeneous photo-Fenton process with zerovalent iron nanoparticles for degradation of toluene in aqueous solution. *Catal. Commun.* **2023**, *183*, No. 106767.
(75) Luo, Z.; Chatterjee, N. Kinetics of oxidation of Cr(III)-organic complexes by H_2O_2. *Chem. Speciation Bioavailability* **2010**, *22*, 25−34.
(76) Mohammadi, S.; Pourakbar, L.; Moghaddam, S. S.; Popović-Djordjević, J. The effect of EDTA and citric acid on biochemical processes and changes in phenolic compounds profile of okra (*Abelmoschus esculentus* L.) under mercury stress. *Ecotoxicol. Environ. Safety* **2021**, *208*, No. 111607.
(77) Batagoda, J. H.; Hewage, S. D. A.; Meegoda, J. N. Remediation of heavy-metal-contaminated sediments in USA using ultrasound and ozone nanobubbles. *J. Environ. Eng. Sci.* **2019**, *14* (2), 130−138.
(78) Fagan, W. P.; Weavers, L. K. Sonochemical Remediation of Pollutants in Soils and Sediments. *Encyclopedia Water: Sci., Technol., Soc.* **2019**, 1−21.

https://doi.org/10.1021/acsengineeringau.4c00011
ACS Eng. Au XXXX, XXX, XXX−XXX